Thermodynamic properties of a lattice model of aqueous mixtures

Radhika Sharma and Deepak Kumar
School of Physical Sciences, Jawaharlal Nehru University, New Delhi 10067, India
(Received 16 March 1998)

The thermodynamic anomalies of water have been studied for a long time by statistical models that incorporate the effects of hydrogen bonding in a qualitative manner by adding certain orientational degrees of freedom. In this paper, we study how these anomalies are carried over to aqueous mixtures, in which the other component molecules form van der Waals bonds with water molecules as well as among themselves. For this purpose we adapt a recent model due to Sastry *et al.*, which is quite successful in exhibiting these anomalies for pure water. In particular, we have studied how anomalous behavior of density and compressibility varies with composition over a range of temperatures and pressures. We have also obtained a few typical phase diagrams for these mixtures. [S1063-651X(98)11709-9]

PACS number(s): 64.70.Ja, 05.70.Ce, 64.60.My, 82.60.Lf

I. INTRODUCTION

Water [1] has long evoked wide theoretical interest because of its various peculiar physical properties. The most widely studied peculiar properties include the following: (a) the density anomaly, i.e., the density of water is maximum at 4 °C, and its thermal expansivity α_P is negative below 4 °C in some temperature and pressure range. (b) The isothermal compressibility K_T increases with decrease in temperature below a certain temperature (50 °C at normal pressure). (c) The constant-pressure specific heat C_p of water is rather large and also increases as the temperature is lowered below some value. All these anomalies are further enhanced in the supercooled or metastable regions of water.

There is a general agreement on the microscopic origin of these peculiarities. They have been attributed to the presence of a hydrogen bond (HB) network in water. The experimental data [2] as well as the detailed microscopic results provided by computer simulations [3–6] seem to suggest that liquid water is a broken network of HBs where there are regions of strong linear HBs interspersed with regions of weaker bonding. The strongly bonded or the low energy regions are characterized by tetrahedral coordination, i.e., each oxygen atom is surrounded by four hydrogen atoms (of the neighboring molecules, thus forming a network) located at the corners of a regular tetrahedron. The formation of HBs between two water molecules is possible only when the two are properly oriented with respect to each other. The hydrogen bonding thus leads to freezing of orientational degrees of freedom. Hence the HB regions are characterized by low entropy. The open tetrahedral geometry gives the hydrogen-bonded regions of water its low local density. The ground state of the hydrogen-bonded water characterized by an open low density structure of low entropy makes ice less dense than liquid water.

The water molecules also have van der Waals (vW) interactions, which are weaker than HBs and are orientationally independent. These interactions acting alone would lower the energy of high density configurations. The weakly bonded regions are characterized by a higher local density and higher molecular mobility. The molecules in the high density regions also have significantly larger orientational entropy compared to those in the low density regions [6]. The high density configurations though have higher internal energy yet are more stable at high temperatures as the contribution of orientational entropy to free energy partially compensates their higher energy as well as the lower configurational entropy.

Although there is general agreement over the microscopic origin of these anomalies, the issue of the thermodynamic behavior resulting from this microscopic behavior is still unresolved. We have attempted to gain some understanding of these issues by studying aqueous mixtures. The aqueous mixtures are important in their own right, but they can also elucidate the role of hydrogen bonding in a larger context.

Thermodynamic properties of mixtures depend mainly on the nature of interactions among its various constituents. The various issues that can be addressed are as follows:

(1) Density anomaly: The temperature of maximum density (TMD) results from a complex interplay of two kinds of bonding in water, namely, vW bonding, which favors denser states and the hydrogen bonding that favors open structures with lower density. Further, the formation of HBs locks up orientational degrees of freedom. Thus, entropically also there is a competition between orientational entropy and configurational entropy. For vW bonded high density structure one gains orientational entropy but may lose in configurational entropy. On the other hand the reverse happens for the HB structure. Thus formation of mixture by addition of the other component (molecules other than water molecules) will have an effect on the structure of water resulting in a consequent shift in TMD. It is known [7] that the addition of entities that result in breaking of HBs thereby reducing the excess volume associated with the open structure of HB regions of water causes the TMD to shift towards the low temperature side. The reverse may happen for the molecules that form HBs with water molecules or among themselves. Thus the nature of bonding (e.g., vW, HB) between the water molecules and the molecules of the other component of the mixture could have a large effect on the density anomaly.

(2) Anomalies in response functions: The effect that the addition of other components to water has on the isothermal compressibility K_T, isobaric heat capacity C_p, etc. could

also provide insight into the thermodynamic behavior of water.

(3) Supercooled water: Thermodynamic anomalies of water become more pronounced on supercooling. Among the interpretations of this behavior is a postulate put forth by Speedy [8,9]. This postulate, called the stability limit conjecture (SLC), predicts that in the P-T plane there should exist a continuous spinodal curve (locus of limits of stability) bounding the supercooled, stretched (in negative pressure region), and superheated states. This line marks the points in the P-T phase diagram where the metastable state of liquid water becomes thermodynamically unstable. The existence of such a curve towards the supercooled side cannot be experimentally verified as the homogeneous nucleation occurs above this temperature and the instability temperature, which is $-45\,^{\circ}\mathrm{C}$ at atmospheric pressure, is not accessible. The addition of another component often results in lowering of freezing and boiling points by a considerable amount. This in principle can make the instability temperature more accessible and provide a way to examine the conjecture. But this is only possible if the addition of the other component does not also lower the instability temperature or raise the homogenous nucleation temperature.

(4) Study of phase diagrams of binary mixtures can also reveal the effect of the addition of the other component on the entropy of the system. In ordinary substances, i.e., substances without HB, at high temperatures it is the entropy of mixing that favors the system to exist in homogeneously mixed state. At low temperatures when the internal energy is the dominating influence on free energy, demixing of phases is favored.

In the case of aqueous mixtures the system has extra configurational entropy on account of the orientational degrees of freedom. At the simplest level, depending on their interaction with water molecules, the impurities can either break HB's, thereby releasing the orientational degrees of freedom, or conversely they can lock up these degrees of freedom by forming stronger HB's with water or among themselves. But for certain impurities water exhibits more complex behavior. The prime example is the clatharate structures in ice, which are distortions of hexagonal structure to cubic forms, by forming cages that accommodate these impurities. In the liquid state also for certain impurities large complexes are formed involving several water molecules with a single impurity molecule [7].

There have been a good many statistical mechanical studies of the thermodynamics of water. As most of the peculiarities of water are due to the directional nature of the HB any good model should incorporate the following features: (1) The low temperature state (ground state) of the system should have an open, low density structure like that of ice. (2) Linear HBs can form between two molecules only when (a) local configuration is open and (b) the participating molecules are properly oriented. (3) Increase in local density with respect to the open structure must result in an increase in the (a) local energy and (b) local entropy. Though the number of models put forth in various studies is large, no single model to date has been able to satisfactorily account for the thermodynamic behavior of water over the entire range of temperature from the supercooled region to the critical temperature. For the metastable or supercooled region there are mainly two thermodynamic scenarios that rely on distinct mechanisms to explain anomalous behavior. One is the stability limit conjecture due to Speedy [8,9,10–12] discussed above. Here anomalous behavior of isothermal compressibility and isobaric heat capacity comes from the fact that both these quantities must diverge at the spinodal. The retracing of the spinodal is argued to be a thermodynamic consequence of the negative sloping of the locus of density maxima (TMD). The other scenario is due to Poole *et al.* [13], who argue that a novel, metastable low temperature critical point is responsible for water's anomalous behavior. They have also observed that the slope of TMD does not remain negative, but changes sign at negative pressures. This change in sign of the slope removes the thermodynamic requirement for the spinodal to retrace.

Many lattice models have been proposed to explain the properties of water. Bell [14] proposed a model with molecules centered on the sites of a body-centered cubic lattice; each molecule could be oriented in 12 ways. In addition to a favorable bonding energy, the model included an attractive first-neighbor interaction and three-body repulsion, which discourages close packing. Bell solved the problem in a quasichemical approximation and he obtained the density maxima. A slight variation of Bell's model [14] was proposed by Meijer *et al.* [15], who introduced a second neighbor repulsion instead of the three-body force used by Bell. The repulsive next nearest neighbor pairs are included to prevent close packing. In this model also the density anomaly appears along with a negatively sloped melting curve between the liquid and a less dense icelike phase.

Borick and Debendetti [16], using the model of Meijer *et al.* [15], have thoroughly investigated the equilibrium and stability behavior of the model in an improved approximation. Their results include quantitative parameter mapping of the phase behavior and characterization of density anomalies and stability limits. Sastry *et al.* [17] have introduced a model to incorporate the open structure on a lattice partitioned into two sublattices A and B. In the ground state, one of the sublattices is completely occupied and the other is empty. The orientational degrees of freedom are incorporated by associating a Pott's variable σ with every occupied site. This Pott's variable σ_i can take q values out of which only one is associated with the orientation favoring hydrogen bonding. Sastry *et al.* [17] have solved this model in the mean-field approximation and have reported waterlike phase behavior, density maxima, and a retracing spinodal.

In a later study, however, Sastry *et al.* [18] presented arguments that establish that anomalies of water may not necessarily depend on singular behavior in the metastable region. They show that the presence of a negatively sloped TMD implies an isothermal compressibility, which must increase with decreasing temperature. They have also used a lattice-gas model that captures some of the crucial features of water (like density maximum) in a simple statistical way. This model exhibits behavior qualitatively similar to that observed in molecular dynamics simulations of water [13]. In this model the orientational degree of freedom is represented by a Potts variable at each lattice bond. This is the model that we found very useful for discussing aqueous mixtures. The model is [18]

$$\mathcal{H}=\frac{H}{k_BT}=-J\sum_{\langle ij\rangle} n_in_j-\delta J\sum_{\langle ij\rangle} n_in_j\delta_{\sigma_{i,j}\sigma_{j,i}}. \tag{1}$$

In Eq. (1) n_i is the occupancy variable at a site i of the lattice such that $n_i=1$ for every occupied site and $n_i=0$ for every vacant site. The Potts variable σ_{ij} defines the orientation of molecule i with respect to molecule j and can take q values. J is the vW interaction energy and $J+\delta J$ is the energy due to HB formation. k_B is Boltzmann's constant and T is the temperature. Clearly, as far as the orientation variables are concerned the model is a gross simplification, as it ignores the correlations between the variables σ_{ij_1}, σij_2, . . . , i.e., between the bond variables originating from the same site. A more appropriate, but considerably more difficult, model is that of Vause and Walker [19]

$$\mathcal{H}=\frac{1}{2}\sum_{\langle ij\rangle} n_in_j[K_2+(K_1-K_2)\delta_{\sigma_i\sigma_j}], \tag{2}$$

where n_i is the usual occupancy variable, σ_i takes q values, K_1 is the energy of the HB, and K_2 is the energy of the vW bond. Under a simple approximation this model also leads to similar results. Apart from the directional nature (orientation dependence) another important feature of HB's is the low local density accompanying every HB formation. This feature of HB's is crucial for density anomaly of water. The model of Sastry *et al.* tries to achieve this goal in a simple manner by defining an interaction dependent volume at each lattice bond ij. The total volume of the system is then the sum of the specific volume at each lattice bond, which is expressed in terms of an interaction dependent contribution to volume $v_{i,j}$. An extra volume is associated with every HB interaction, so that $v_{i,j}=v_1+\delta v$, where δv is the extra volume associated with HB and $v_{ij}=v_1$ otherwise. Thus the total volume V becomes

$$\begin{aligned} V&=\sum_{\langle i,j\rangle}(v_1+\delta v n_in_j\delta_{\sigma_{i,j},\sigma_{j,i}})\\ &=\frac{N_0zv_1}{2}+\delta v\sum_{\langle i,j\rangle} n_in_j\delta_{\sigma_{i,j},\sigma_{j,i}}, \end{aligned} \tag{3}$$

where N_0 is the number of lattice sites and z is the coordination number.

It can be seen from Eqs. (1) and (3) above that the configuration of water molecules with strong HB interactions defines a state of low local energy and low density while that with weak vW interactions defines a state of high local energy and density. For this type of system the entropy density is a sum of a configurational part and an orientational part. The free energy for this model is calculated in the mean-field (MF) approximation. The partition function is calculated in a special grand canonical ensemble, in which one sums over not only particle number but also the volume, i.e., the number of lattice sites. By performing a sum over the Pott's variable $\sigma_{i,j}$ or the orientational degrees of freedom, the partition function is reduced to an effective lattice gas partition function with temperature dependent interaction parameters. The results of this model include anomaly in density and isothermal compressibility. The locus of temperature of maximum density (TMD) is found to change slope from negative to positive, thus removing the thermodynamic necessity of a retracing spinodal. The locus of temperature of compressibility extrema (TEC) has also been explored in detail. The main result of the study is the absence of retracing spinodal bounding the supercooled metastable state of water.

There have been many studies on aqueous mixture and their properties in physical chemistry. The statistical mechanical studies are limited to exploring the phase diagrams of binary mixtures in general, including hydrogen-bonded mixtures. The most well studied of all the models of binary mixtures is the lattice-gas model of Walker and Vause (WV) [19,20]. The WV model is quite successful in understanding the closed loop phase diagrams of binary mixtures.

The WV model has further been explored by Goldstein and Walker [21] and Goldstein [22]. Caflish and Walker [23] have tried to modify the WV model to incorporate vaporization in the model. These studies, however, have not considered the density and other anomalies of water.

The scope of this study is limited to examining the following simpler points about aqueous mixtures: (a) the effect of the other component on the orientational entropy of the system and its interplay with the usual entropy of mixing, (b) the study of the volume anomaly associated with HB's. In this paper we study only those mixtures in which the second component molecules form only vW bonds with water molecules and among themselves. In the next section we set up a lattice gas model for a binary (AB) mixture, in which one type of molecule (say *AA*) has a possibility of HB formation. We incorporate waterlike properties through the model of Sastry *et al.* as given in Eqs. (1) and (3). We then make a mean-field approximation and obtain the free energy and the equation of state for the system. These equations are then solved numerically to get the various thermodynamic properties and phase diagrams. The numerical results are presented in Sec. III and Sec. IV concludes this paper with a brief discussion of the results.

II. LATTICE MODEL AND FREE ENERGY

In this section we present a lattice gas model for aqueous mixtures (say *AB*) in which the water molecules *(A)* are bonded to other component molecules *(B)* through vW binding. The molecules of the other component (other than water) of the mixture form only vW bonds with each other as well as with water molecules. Further there are no orientational degrees of freedom associated with *B* molecules, unlike water molecules. A binary mixture could be described in terms of occupancy variables P_i^A and P_i^B such that $P_i^{A(B)}=1$ if the ith cell is occupied by the *A (B)* atom (molecule) and zero otherwise. The *AA* interactions in our model are both vW and HB type. Our model Hamiltonian is

$$\begin{aligned} \mathcal{H}=-\sum_{ij}\ [&(J_{AA}+\delta J_{AA}\delta_{\sigma_{i,j},\sigma_{j,i}})P_i^AP_j^A\\ &+J_{AB}(P_i^AP_j^B+P_i^BP_j^A)+J_{BB}P_i^BP_j^B], \end{aligned} \tag{4}$$

where J_{AA}, J_{AB}, and J_{BB} represent the strength of vW interaction between particle pairs *AA*, *AB*, and *BB*, respectively

and δJ_{AA} is the additional energy due to HB formation. Inclusion of orientational degrees of freedom is by associating Pott's variable.

To account for the fact that each HB is associated with increased local volume, we follow exactly the same procedure as described by Sastry *et al.* [18]. We define an interaction dependent volume at each lattice site i. The total volume of the system then becomes

$$V=\sum_{\langle ij\rangle}(v_1+\delta v\,\delta_{\sigma_{ij}\sigma_{ji}}P_i^AP_j^A)$$
$$=N_0v_0+\delta v\sum_{\langle ij\rangle}\delta_{\sigma_{ij}\sigma_{ji}}P_i^AP_j^A. \tag{5}$$

In the above equation, $v_0=v_1z/2$. The total volume of the system thus depends on the number of HB's present.

For evaluating the partition function for the above Hamiltonian we work in an ensemble in which both the volume of the system as well as the number of particles can be variable. Such an ensemble is necessary because the volume is a dynamical variable here and one is interested in tracking the density anomaly. The partition function $\mathcal{Z}$ in this ensemble is a function of only the intensive parameters pressure P, temperature T, and chemical potentials μ_A and μ_B for the two species, respectively:

$$\mathcal{Z}(P,T,\mu_A,\mu_B)=\sum_{N_0}\sum_{S_i,\sigma_{ij}}\times\exp[-\beta(H+PV-\mu_AN_A-\mu_BN_B)], \tag{6}$$

where $\beta=1/k_BT$. As noted by Sastry *et al.*, although the corresponding free energy $\mathcal{Y}(P,T,\mu_A,\mu_B)$ is identically zero, it is still useful for deriving the equilibrium properties. The fact that partition function $\mathcal{Z}\equiv1$ provides an additional relationship for evaluation of dependent variables [18]. Substituting the expression for H, V in Eq. (6), the partition function becomes

$$1=\sum_{N_0}\exp(-\beta Pv_0N_0)\sum_{S_j}\sum_{\sigma_{ij}}\sum_{\{S_i\}}\exp\Bigg[\beta\sum_{i,j}\{J_{AA}P_i^AP_j^A+J_{AB}(P_i^AP_j^B+P_i^BP_j^A)+J_{BB}P_i^BP_j^B\}$$
$$+\beta(\delta J_{AA}-P\delta v)\sum_{i,j}P_i^AP_j^A\delta_{\sigma_{i,j},\sigma_{j,i}}+\beta\sum_i(\mu_AP_i^A+\mu_BP_i^B)\Bigg]. \tag{7}$$

In the above equation the summation over $\{\sigma_{i,j}\}$ variables is to be carried out for individual bonds, which can be done exactly here as the partition sum breaks up into independent factors. This summation including the chemical potential factor, i.e., $\exp[(\mu_A/z)(P_i^A+P_j^A)]$ for one bond, depends on occupancy variable P_i^A and P_j^A in the following manner:

$$\sum_{\sigma_{i,j},\sigma_{j,i}}\{1+[\exp(\beta K_pP_i^AP_j^A)-1]\delta_{\sigma_{i,j},\sigma_{j,i}}\}=\begin{cases}1 & \text{if } P_i^A=P_j^A=0\\ q\,\exp(\beta\mu_A/z) & \text{if } P_i^A+P_j^A=1\\ q^2\exp(2\beta\mu_A/z)[1+(1/q)(\exp(\beta K_p)-1)] & \text{if } P_i^A=P_j^A=1,\end{cases} \tag{8}$$

where $K_p=(\delta J_{AA}-P\delta v)$. Thus, our partition function takes the form

$$\mathcal{Z}=1=\sum_{N_0}\exp(-\beta Pv_0N_0)\sum_{\{S_i\}}\exp\Bigg[\beta\sum_{i,j}\Bigg\{\Bigg(J_{AA}+k_BT\ln\Bigg[1+\frac{1}{q}(\exp(\beta K_p)-1)\Bigg]\Bigg)P_i^AP_j^A$$
$$+J_{AB}(P_i^AP_j^B+P_i^BP_j^A)+J_{BB}P_i^BP_j^B\Bigg\}+\beta\sum_i\Bigg(\mu_A+\frac{k_BT}{z}\ln(q)\Bigg)P_i^A+\mu_BP_i^B\Bigg\}. \tag{9}$$

For convenience of calculation, we introduce a three state spin variables $S_i=\pm1,0$ in terms of which

$$P_i^A=\tfrac{1}{2}(S_i^2+S_i),$$
$$P_i^B=\tfrac{1}{2}(S_i^2-S_i), \tag{10}$$

such that $S_i=1(-1)$ corresponds to a lattice site i being occupied by molecule *A(B)* and $S_i=0$ corresponds to a vacant lattice site. Thus Eq. (9) takes the form

$$1=\sum_{N_0}\exp(-\beta Pv_0N_0)\sum_{\{S_i\}}\exp\Bigg[\beta\sum_{\langle ij\rangle}\{K_eS_i^2S_j^2+L_e(S_i^2S_j+S_iS_j^2)+J_eS_iS_j\}+\beta\sum_i(D_eS_i^2+H_eS_i)\Bigg], \tag{11}$$

where the various interaction parameters are

$$K_e=\frac{1}{4}\left\{(J_{AA}+2J_{AB}+J_{BB})+k_BT\ \ln\left[1+\frac{1}{q}(\exp(\beta K_p)-1)\right]\right\},$$

$$L_e=\frac{1}{4}\left\{(J_{AA}-J_{BB})+k_BT\ \ln\left[1+\frac{1}{q}(\exp(\beta K_p)-1)\right]\right\},$$

$$J_e=\frac{1}{4}\left\{(J_{AA}-2J_{AB}+J_{BB})+k_BT\ \ln\left[1+\frac{1}{q}(\exp(\beta K_p)-1)\right]\right\}, \tag{12}$$

$$D_e=\frac{\mu_A+\mu_B}{2}+\frac{k_BT}{2z}\ln(q),$$

$$H_e=\frac{\mu_A-\mu_B}{2}+\frac{k_BT}{2z}\ln(q).$$

Now we use the mean-field approximation to evaluate the partition function [24]. For this we define two order parameters as follows:

$$Q=\langle S_i^2\rangle,$$
$$\tilde{M}=\langle S_i\rangle, \tag{13}$$

where $\langle\ \rangle$ corresponds to ensemble average. The order parameter Q corresponds to the average particle density and $\tilde{M}$ to the concentration difference between the two species.

In the mean-field approximation the partition function becomes

$$1=\sum_{N_0}\exp(-\beta P v_0 N_0)\exp\left[-\frac{\beta N_0 z}{2}(K_eQ^2+2L_eQ\tilde{M}+J_e\tilde{M}^2)\right]$$
$$\times[1+\exp\{\beta(zK_eQ+zL_e\tilde{M}+D_e)\}2\cosh\{\beta(zJ_e\tilde{M}+zL_eQ+H_e)\}]^{N_0}. \tag{14}$$

This expression has the form

$$1=\sum_{N_0}\exp[-\beta P v_0 N_0-N_0\beta A(Q,\tilde{M},\beta,D,H)]. \tag{15}$$

The sum over N_0 is dominated by just one term, which maximizes the exponent, i.e.,

$$1=\exp\{-\beta[Pv_0+A(Q,\tilde{M},\beta,D,H)]\overline{N_0}\}, \tag{16}$$

where $\overline{N_0}$ is determined from the equation

$$Pv_0+A+\left[\frac{\partial A}{\partial Q}\frac{\partial Q}{\partial N_0}N_0+\frac{\partial A}{\partial\tilde{M}}\frac{\partial\tilde{M}}{\partial N_0}N_0\right]_{\overline{N_0}}=0. \tag{17}$$

However, Q and $\tilde{M}$ are variational parameters, which are to be determined from the condition

$$\frac{\partial A}{\partial Q}=0,$$
$$\frac{\partial A}{\partial\tilde{M}}=0. \tag{18}$$

Thus

$$Pv_0=-A$$
$$=-\frac{z}{2}(K_eQ^2+2L_eQ\tilde{M}+J_e\tilde{M}^2)$$
$$+k_BT\ \ln\{1+2\exp[\beta(zK_eQ+zL_e\tilde{M}+D_e)]$$
$$\times\cosh[\beta(zJ_e\tilde{M}+2L_e\tilde{M}+H_e)]\}. \tag{19}$$

The variational equations yield

$$Q=\frac{2\exp(\beta d_1)\cosh(\beta d_2)}{1+2\exp(\beta d_1)\cosh(\beta d_2)},$$
$$\tilde{M}=\frac{2\exp(\beta d_1)\sinh(\beta d_2)}{1+2\exp(\beta d_1)\cosh(\beta d_2)}, \tag{20}$$

where $d_1=(zK_eQ+zL_e\tilde{M}+D_e)$ and $d_2=(zJ_e\tilde{M}+zL_eQ+H_e)$.

The free energy in Eq. (19), which is a function of D_e and H_e, is not the most appropriate potential for getting the physical properties of mixtures with fixed concentration. So we perform a Legendre transformation to obtain the free energy $G(P,T,N,M)$, where the independent variable $D=D_e-(k_BT/2z)\ln(q)$ and $H=H_e-(k_BT/2z)\ln(q)$ have been replaced by particle number $N=N_0Q$ and concentration difference $M=\tilde{M}/Q$. Note that

$$Q=\frac{N_A+N_B}{N_0},$$

$$\tilde{M}=\frac{N_A-N_B}{N_0}, \tag{21}$$

$$M=\frac{N_A-N_B}{N_A+N_B},$$

where $N_{A(B)}$ is the number of *A(B)* molecules. G is given by

$$\begin{aligned} G(P,T,N,M)&=\mathcal{Y}(P,T,D,H)+D(N_A+N_B)+H(N_A-N_B)\\ &=N(D+HM). \end{aligned} \tag{22}$$

Denoting

$$g(P,T,M)=\frac{1}{N}G(P,T,N,M),$$

we obtain the most convenient free-energy potential for our purpose, viz.,

$$\begin{aligned} g(P,T,M)=&-zQ(K_e+2L_eM+J_eM^2)\\ &+k_BT\left\{\ln\left[\frac{Q}{1-Q}\right]+\frac{1+M}{2}\ln\left(\frac{1+M}{2}\right)\right.\\ &\left.+\frac{1-M}{2}\ln\left(\frac{1-M}{2}\right)\right\}-\frac{k_BT}{z}(1+M)\ln(q). \end{aligned} \tag{23}$$

Eliminating D and H from Eq. (19) gives us the expression for pressure

$$P=-\frac{z}{2}Q^2(K_e+2L_eM+J_eM^2)-k_BT\ln(1-Q). \tag{24}$$

The free-energy expression for g contains the auxiliary variable Q, which must be eliminated by use of the expression for pressure P. To perform the calculations, one obtains from Eq. (24) the values of Q for given values of P, T, and M. Note that Q is not a single-valued function of P, T, and M. Depending on the parameter values one obtains one, two, or three solutions giving rise to as many branches of free energy. For the purpose of studying the thermodynamic anomalies in the supercooled regime it is the branch corresponding to the density anomaly that is of interest. This branch may not always be the lowest free-energy branch. For the purpose of studying the concentration-temperature phase diagrams, the lowest branch gives the appropriate free energy.

The volume of the system can be derived using the relation $v=\partial g/\partial P$, to obtain

$$v=\frac{v_0}{Q}+\frac{Q}{2}\frac{\delta v z}{[1+(q-1)\exp(-\beta K_P)]}\frac{(1+2M+M^2)}{4}. \tag{25}$$

Equations (23), (24), and (25) are sufficient for the purpose of studying various thermodynamic properties of aqueous mixtures.

We explore the density anomaly and thermodynamic response functions, i.e., thermal expansivity $(\alpha=(1/v)\,\partial v/\partial T)$, isothermal compressibility $[K_T=-(1/v)(\partial v/\partial P)_T]$ and isobaric heat capacity $[C_P=-T(\partial^2 g/\partial T^2)_P]$. The expressions for these quantities are given below:

$$\begin{aligned} \alpha=\frac{1}{v}\Bigg[&\left(-\frac{v_0}{Q^2}+\frac{z\,\delta v}{2}M_1D_1\right)\\ &\times\left[\frac{zQ^2}{2}\left(G_1-\frac{K_PD_1}{T}\right)M_1+k_B\ln(1-Q)\right]T_1\\ &-\frac{Q}{2}M_1\left(\delta v z(q-1)\beta K_P\exp(-\beta K_P)\frac{D_1^2}{T}\right)\Bigg], \end{aligned} \tag{26}$$

where

$$M_1=\left(\frac{1+M}{2}\right)^2,$$

$$D_1=\frac{1}{1+(q-1)\exp(-\beta K_P)},$$

$$G_1=\ln\left[1+\frac{1}{q}[\exp(\beta K_P)-1]\right],$$

and

$$T_1=\left[\frac{(1-Q)}{k_BT-zQ(1-Q)(K_e+2L_eM+J_eM^2)}\right].$$

Using the above definitions we can write the expression for isothermal compressibility

$$\begin{aligned} K_T=\frac{1}{v}\Bigg[&\left(\frac{v_0}{Q}-\frac{\delta v z}{2}M_1D_1\right)^2T_1\\ &+[\delta v^2\beta Q z(q-1)\exp(-\beta K_P)M_1D_1^2]. \end{aligned} \tag{27}$$

Similarly, the isobaric heat capacity is

$$\begin{aligned} C_P=\frac{k_B^2T}{Q^2}\Bigg[&\left(\ln(1-Q)+\frac{zQ^2}{2}(G_1-\beta K_PD_1)M_1\right]^2T_1\\ &+\left(\frac{zQ}{2T}\beta K_P^2(q-1)\exp(-\beta K_P){D_1}^2M_1\right). \end{aligned} \tag{28}$$

III. NUMERICAL RESULTS

A. Thermodynamic properties

Using the equations presented in the previous section, we study the thermodynamic properties of the system described above. We shall focus on the concentration dependence of anomalous properties like TMD curve, α_P, K_T, and C_P.

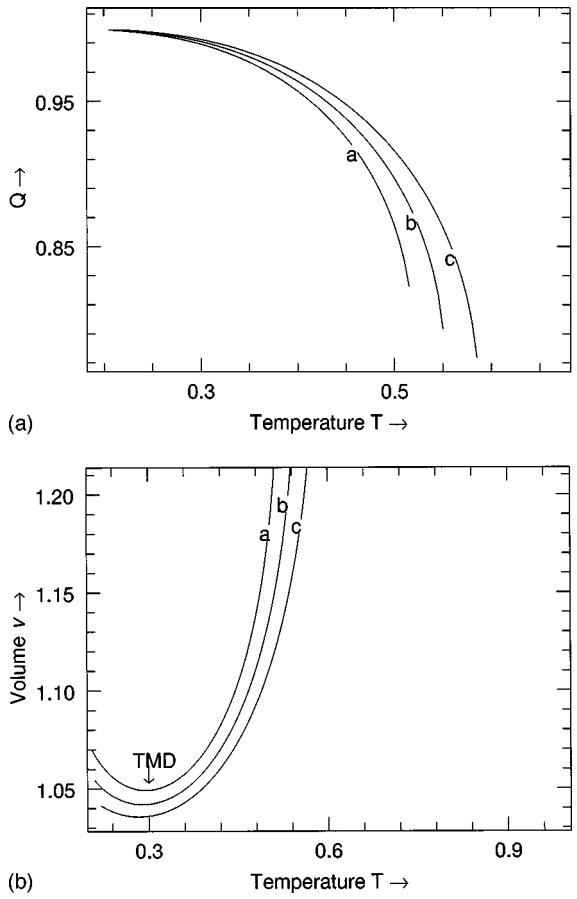

FIG. 1. (a) The Q vs T curve. The three curves shown are for different fixed pressures: curve *a*, $P=-0.15$, curve *b*, $P=-0.10$, and curve *c*, $P=-0.05$. It can be seen that these curves do not have any extrema. (b) The volume v vs T curves where the symbols *a*, *b*, and *c* mean the same as in (a). The arrow indicates the temperature of minimum volume or maximum density (TMD). The units of various quantities are as follows: Q is dimensionless, T is in the units J_{AA}/k_B, P is in units of J_{AA}/v_0, and v in the units of v_0.

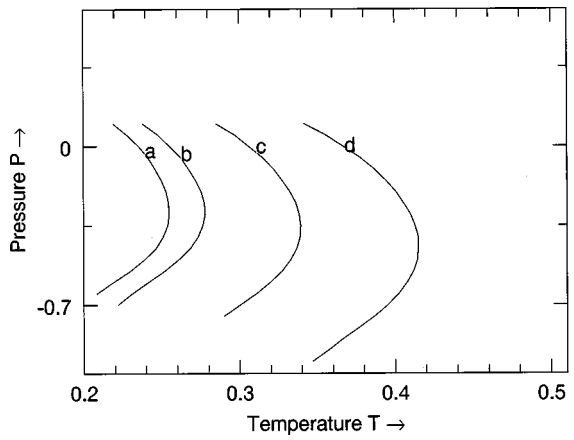

FIG. 2. The locus of the temperature of maximum density TMD for different values of M: curve *a*, $M=0.25$; curve *b*, $M=0.50$; curve *c*, $M=0.75$; and curve *d*, $M=1.00$. Here M is a dimensionless number and the units of T are the same as in Fig. 1.

Our model is successful in reproducing anomalies in density, isothermal compressibility, and thermal expansivity. The data shown are for the choice of parameters $J_{AB}/J_{AA}=0.25$, $J_{BB}/J_{AA}=0.50$, $\delta V/V_0=0.953$, $\delta J_{AA}/J_{AA}=0.25$, $q=100$, and $z=4$. In all the diagrams below P is in the units of J_{AA}/v_0 and T is in the units J_{AA}/k_B.

To get the density anomaly we use Eqs. (24) and (25). We eliminate Q from Eq. (25) using Eq. (24). It should be noted that Q would have represented the density if we had not included the additional volume associated with hydrogen bonds. It is clear from Eq. (25) that the volume is the sum of two terms whose dependence on pressure *(P)* and temperature *(T)* are different. It is the second term that gives rise to the anomalous behavior resulting in a minimum in volume-temperature curve. Figure 1(a) depicts the Q versus T curves for different values of pressure. Though Q is a multiple-valued function we only show the branch that gives rise to anomalous trends in volume. It may be noted that the volume anomaly does not always occur in the lowest free energy branch. This means that the density anomaly is carried over to the supercooled region, which is metastable in the sense that a lower free energy branch also exists at that temperature. In Fig. 1(b) are shown the corresponding volume v versus temperature T curves. It should be noted that there is no density anomaly in the Q versus T curves.

We track the density anomaly, i.e., the temperature of maximum density (TMD) or minimum volume in the v-T plane over a range of pressures. The locus of all such points in the pressure *(P)*–temperature *(T)* plane constitutes what is known as the TMD curve. Since one of our goals in this study was to understand the effect of addition of the other component on the density anomaly, we locate the TMD in the P-T plane for different relative concentrations of the mixture. The curves shown in Fig. 2 correspond to $M=1.0,0.75,0.50,0.25$ (decreasing M in our model corresponds to increasing concentration of the other component of the mixture, as $M=1.0$ corresponds to pure water). It is clear from these curves that as we increase the concentration of the second component (say *B*) the temperature of maximum density moves towards the lower temperature. This shift can be understood as follows: As the concentration of the second component of mixture goes up the number of hydrogen bonds in the mixture go down, resulting in the volume decrease and the release of orientational degrees of freedom. These orientational degrees of freedom lead to an increase in the overall entropy of the system. This increased entropy is responsible for the shift in TMD towards the lower temperature. This result is in accordance with the thermodynamic expectation [7]. Note that the TMD curves do not have a negative slope all through, which as we shall see is consistent with the absence of a retracing spinodal. The anomalous trend in the coefficient of thermal expansion or thermal expansivity α_P is related to the volume or density anomaly. This is clear from the definition of $\alpha_P=(1/v)(\partial v/\partial T)_P$ already given in the last section. The α_P, unlike other normal liquids, becomes negative at the temperature where volume becomes minimum or the density becomes maximum.

In Fig. 3, we show some of the representative curves for α_P versus T curves. Figure 3(a) corresponds to $M=1.0$ and in Fig. 3 (b) we show the curves for $M=0.50$. A comparison of the two figures reveals that the zero-crossing temperature (the temperature below which α_P becomes negative) of the coefficient of thermal expansion has moved towards a lower temperature, a trend similar to that exhibited by the TMD.

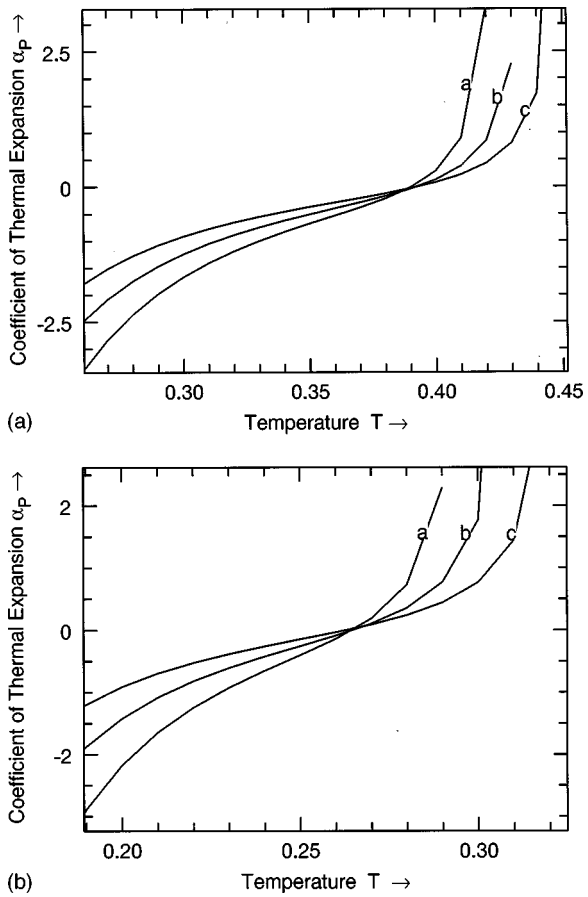

FIG. 3. Coefficient of thermal expansion as a function of temperature for (a) $M=1.00$ for different fixed pressures: curve *a*, $P=-0.38$; curve *b*, $P=-0.34$; and curve *c*, $P=-0.30$; (b) $M=0.50$ for $P=-0.24$ *(a)*, $P=-0.20$ *(b)*, and $P=-0.16$ *(c)*. The temperature of zero crossing is marked in the figure. α_P is in units of k_B/J_{AA}. The units of the rest of the quantities are the same as in Fig. 1.

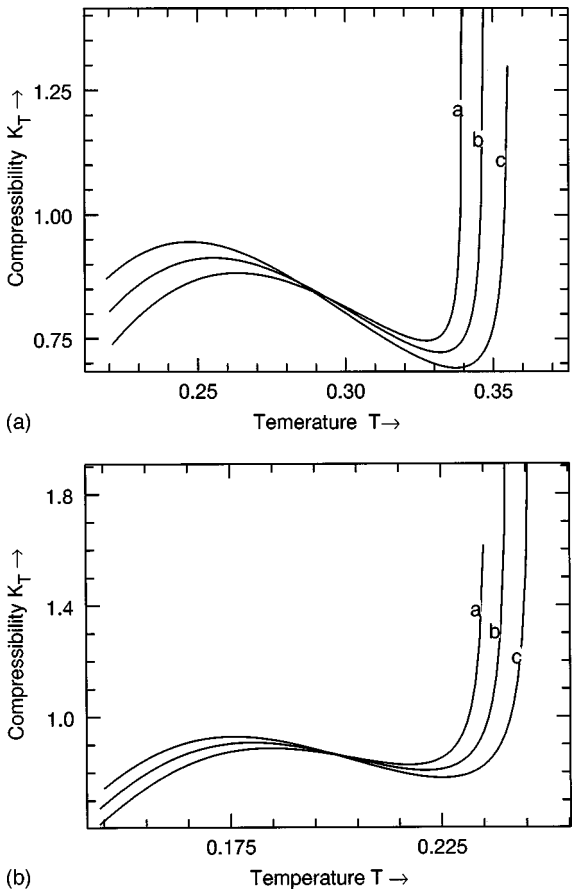

FIG. 4. Isothermal compressibility as a function of temperature for (a) $M=1.0$ the three isobars are for $P=-1.00$ *(a)*, $P=-0.96$ *(b)*, and $P=-0.92$ *(c)*; (b) $M=0.50$ for $P=-0.64$ *(a)*, $P=-0.62$ *(b)*, and $P=-0.60$ *(c)*. It may be noticed that the region of abnormality moves up towards high pressure values. The K_T is in units of v_0/J_{AA} and other units are same as in Fig. 1.

One also notes that the anomaly is enhanced at lower temperatures, which is consistent with the observed behavior.

In Fig. 4, we show the curves for the isothermal compressibility K_T as a function of temperature T. Figure 4(a) shows isothermal compressibility isobars for different pressures for $M=1.0$. Figure 4(b) shows similar curves for $M=0.50$ for different pressure. It was observed that the extremum of the isothermal compressibility moves towards higher pressure. The locus of all the temperatures of K_T minima for different pressures constitutes what is known as the TEC (temperature of extremum of compressibility) curve.

In Fig. 5, the TEC curves for different values of M are compared. It is clear from these curves that as M decreases the TEC moves towards higher pressure and lower temperature. The addition of other components to water also affects its critical point and its phase transition temperatures. This effect can be observed in the pressure *(P)*–temperature *(T)* phase diagrams by tracing the liquid-gas coexistence curves. Figure 6 shows four such coexistence curves corresponding to $M=1.0$, 0.75, 0.50, and 0.25. It can be seen that with the increase in concentration of the other component, the coexistence curves not only move to the low temperature side but also decrease in expanse. The critical point (T_c, P_c) also goes down with M.

The existence of a retracing spinodal in the supercooled region of water is one of the issues that is still debated. According to the two prevailing thermodynamic scenarios [8,13], it is necessary that if the TMD remains negatively

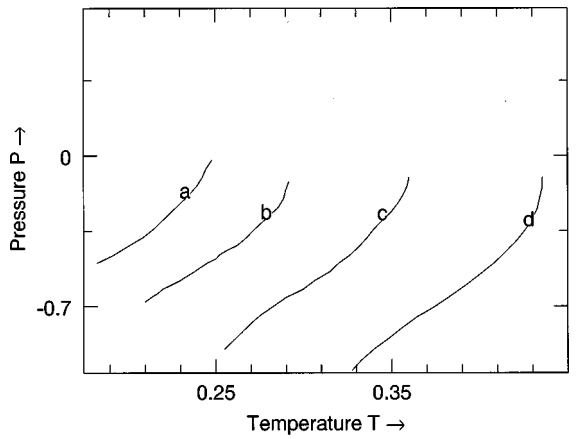

FIG. 5. The locus of compressibility extrema (TEC) in the pressure-temperature plane. The four curves are for $M=0.25$ *(a)*, $M=0.50$ *(b)*, $M=0.75$ *(c)*, and $M=1.00$ *(d)*. As M goes down or the concentration of the second component increases, the expanse of TEC decreases and it moves to the low temperature side.

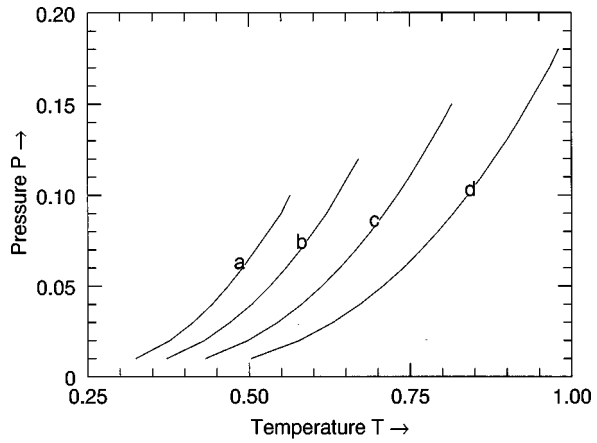

FIG. 6. The liquid-gas coexistence curves the system under study in the pressure-temperature plane for $M=0.25$ *(a)*, 0.50 *(b)*, 0.75 *(c)*, and 1.00 *(d)*. The critical point moves down in temperature and pressure as M decreases.

sloped over the entire range of pressures then the spinodal must retrace at the point of intersection of the two curves or else the TMD must change slope, removing the thermodynamic necessity on the spinodal to retrace. To get the spinodal we track the isothermal compressibility as a function of temperature. For a given pressure the spinodal temperature is the temperature at which $K_T \to \infty$. The spinodal that our model gives is the liquid-gas spinodal, which terminates at the liquid-gas critical point (T_c, P_c). In Fig. 7 we present the spinodals obtained for our model for $M=1.0$, 0.75, 0.50, and 0.25. These spinodals have also been found to follow the same trend as all the other quantities discussed so far. The spinodals also move to the high pressure and low temperature side as M goes down. Thus the model does not display the retracing of spinodal to positive pressures on the low temperature side, as the basic model on which it is based also has this feature.

In Fig. 8 we show a set of representative C_P versus T curves corresponding to the metastable branch of free energy, which shows a density anomaly. These results show that in the parameter range studied by us, the specific heat C_P of the model, unlike K_T, does not exhibit anomalous behavior.

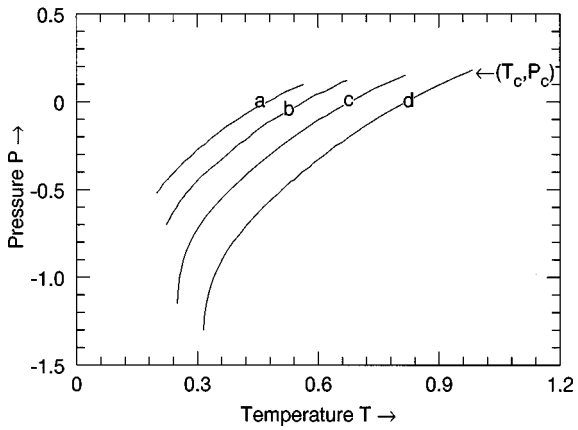

FIG. 7. The spinodal curves in the pressure-temperature plane for $M=0.25$ *(a)*, 0.50,*(b)* 0.75 *(c)*, and 1.00 *(d)*. The response functions K_T and C_P become singular at the spinodal curves.

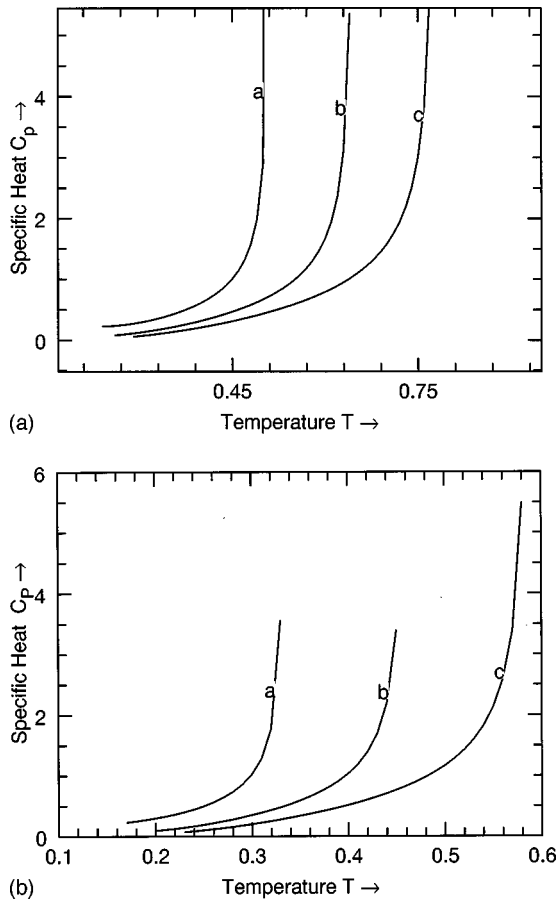

FIG. 8. Isobaric heat capacity C_P as a function of temperature T for (a) $M=1.0$ the different isobars are for $P=-0.50$ *(a)*, $P=-0.25$ *(b)*, $P=-0.05$ *(c)*; and (b) $M=0.50$ curves *a*, *b* and *c* are for the same pressures as in (a). It can be seen that these curves do not show any anomalous behavior. C_P is in the units of k_B.

B. Phase diagrams

We also present the concentration-temperature (M-T) phase diagrams for the aqueous mixture using the model derived in the previous section. To get the phase diagrams, we first obtain solutions for Q for fixed values of P and T. There are in general one to three solutions. The free energy is then obtained for each of these solutions. These are then plotted as a function of concentration variable M for each value of P and T. If the branches do not overlap, the lowest branch corresponds to the equilibrium phase. For a single mixed phase to be stable the free energy of this branch is a globally convex function of the concentration M. When the homogeneously mixed phase is no longer stable, the system decomposes into two coexisting but distinct phases of differing densities and compositions. This is indicated by the intersection of the different branches of free energy. The concentration and densities of the equilibrium phases can be calculated from the free-energy curves by common tangent construction. Sometimes a single phase separates into two phases of different compositions but the same density. This is indicated by the lack of global convexity of the lowest free-energy branch. Depending on the values of the various parameters of the model there is a possibility of the existence of a number of different phases. We here present a few representative situations. The phase diagrams are considered un-

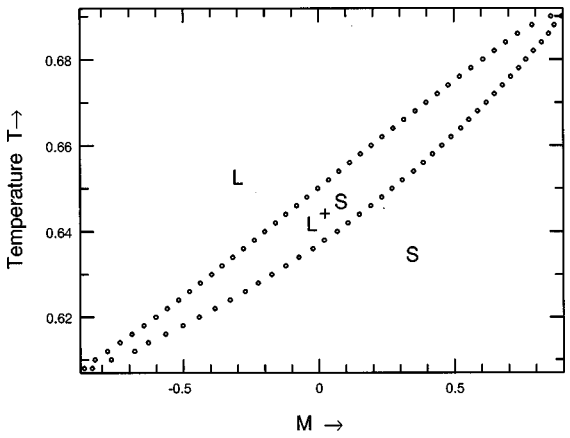

FIG. 9. M vs T phase diagram for $J_{AB}/J_{AA}=5/7$ and $J_{BB}/J_{AA}=3/7$, and $P=0.2/7$.

der the condition of fixed pressure. We denote by L the phase corresponding to a smaller Q value. Since in our model Q does not represent the true density of the system on account of the extra volume resulting from the formation of HB, this phase may or may not be the low density phase. The true density of the phase is calculated by substituting for the value of Q in Eq. (25). The high Q phase is labeled by S. The phases labeled by α and β differ in concentration M but have the same Q values generally in the range of the S phase.

Figure 9 depicts a situation where there is complete miscibility between A and B. The dimensionless interaction parameters and pressure used are $J_{AB}/J_{AA}=5/7$ and $J_{BB}/J_{AA}=3/7$, and $P=0.2/7$. At high temperatures it is the L phase that is stable, as the temperature is lowered there is a possibility of the coexistence of L and S phases. At still lower temperatures it is the S phase that is stable.

In Fig. 10 we show the phase diagram for the interaction parameters and pressure: $J_{AB}/J_{AA}=17/23$ and $J_{BB}/J_{AA}=1.0$, and $P=0.8/23$. Now at low temperatures the demixing of phases is energetically favorable and two phases α and β coexist. At a higher temperature a homogeneously mixed S phase is stable. At a still higher temperature L coexists with the S phase. Above this temperature the mixture exists in a single L phase.

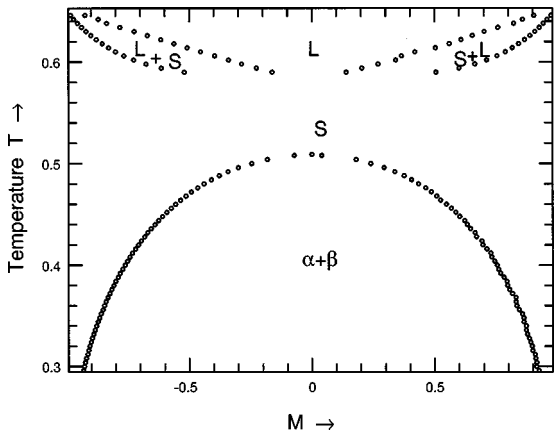

FIG. 10. Phase diagram for $J_{AB}/J_{AA}=17/23$ and $J_{BB}/J_{AA}=1.0$, and $P=0.8/23$.

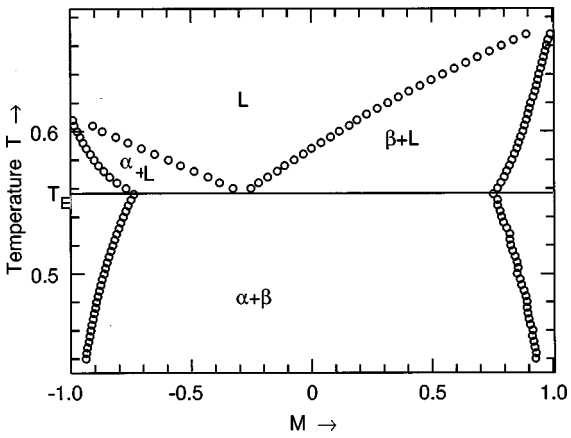

FIG. 11. Phase diagram for $J_{AB}/J_{AA}=40/63$ and $J_{BB}/J_{AA}=19/21$, and $P=2/63$. T_E is the eutectic temperature at which three phases L, α, and β coexist.

Figure 11 shows the phase diagram for the following parameters: $J_{AB}/J_{AA}=40/63$ and $J_{BB}/J_{AA}=19/21$, and $P=2/63$. This diagram is referred to as the eutectic phase diagram. It shows the coexistence of three phases L, α, and β at one temperature T_E. The other phases can be seen in the diagram.

IV. SUMMARY AND DISCUSSION

We now present a brief discussion of our results. We undertook this study to understand how the anomalies of water are affected by the addition of another component to water. The lattice-gas model we used for aqueous mixtures is relevant to those situations in which the other component forms vW bonds with the water molecules. Using this model we studied how the anomalies in density, isothermal compressibility, and thermal expansivity vary with the concentration of the other component. The results are according to our expectation. This type of modelling does not include more complex features that water is known to exhibit, like complex formation or structural alterations as in clatharates.

We also present concentration-temperature phase diagrams. Though we have shown only three phase diagrams, our model is capable of producing many more phase diagrams for different parameter values. For the parameter range explored by us, these phase diagrams are not qualitatively different from mixtures with only van der Waals interactions [25]. We expect that orientational degrees of freedom associated with HB's can produce new kinds of phase diagrams in other situations, such as the closed loop diagrams [19,20], which arise when unlike molecules form stronger HBs, than the like molecules.

To conclude, we have studied aqueous mixtures from statistical mechanical point of view by extending a lattice model of water. These calculations yield several results that need quantitative verification. Such experimental tests would help us to make better models of water, in particular, in understanding the quantitative role of hydrogen bonds. These also suggest that detailed exploration of phase diagrams of aqueous mixtures can also be a fruitful way of probing basic properties of water.

[1] For a complete account of water, see *Water—A Comprehensive Treatise*, edited by F. Franks (Plenum, New York, 1971–1981), Vols. 1–7.

[2] E. Grunwald, J. Am. Chem. Soc. **108**, 5719 (1986); A. H. Narten and H. A. Levy, Science **165**, 447 (1969); L. Bosio, S. H. Chen, and J. Teixeira, Phys. Rev. A **27**, 1468 (1983); P. A. Giguere, *ibid.* **35**, 4835 (1987); G. E. Walrafen, M. S. Hokmabadi, W. H. Yang, Y. C. Chu, and B. Monosmith, J. Phys. Chem. **93**, 2909 (1989).

[3] A. Geiger, P. Mausbach, and J. Schnitker, in *Water and Aqueous Solutions*, edited by G. W. Neilson and J. E. Enderby (Adam Hilger, Bristol, 1986); A. Geiger, A. Rahman, and F. H. Stillinger, J. Chem. Phys. **70**, 273 (1979); A. Geiger and P. Mausbach, in *Hydrogen Bonded Liquids*, edited J. Dore and J. Teixeira (Kluwer Academic, Dordrecht, 1990).

[4] H. Tanaka and I. Ohmine, J. Chem. Phys. **87**, 6128 (1987); I. Ohmine, H. Tanaka, and P. G. Wolynes, *ibid.* **89**, 5852 (1988); H. Tanaka and I. Ohmine, *ibid.* **91**, 6318 (1989).

[5] F. H. Stillinger and A. Rahman, J. Chem. Phys. **60**, 1545 (1974); M. Mezei and D. L. Beveridge, *ibid.* **74**, 622 (1981); R. J. Speedy, J. D. Madura, and W. L. Jorgersen, J. Phys. Chem. **91**, 909 (1987); D. A. Zichi and P. J. Rossky, J. Chem. Phys. **84**, 2814 (1986).

[6] F. Sciortino, A. Geiger, and H. E. Stanley, Phys. Rev. Lett. **65**, 3450 (1990); Nature (London) **354**, 218 (1991); J. Chem. Phys. **96**, 3857 (1992); F. Sciortino, in *Correlations and Connectivity*, edited by H. E. Stanley and N. Ostrowsky (Kluwer Academic, Dordrecht, 1990).

[7] F. Franks, in *Water* (Royal Society of Chemistry Press, London, 1984).

[8] R. J. Speedy, J. Phys. Chem. **86**, 986 (1982).

[9] R. J. Speedy, J. Phys. Chem. **86**, 3002 (1982).

[10] P. G. Debenedetti and M. C. D'Antonio, J. Chem. Phys. **84**, 3339 (1986).

[11] P. G. Debenedetti and M. C. D'Antonio, J. Chem. Phys. **85**, 4005 (1986).

[12] M. C. D'Antonio and P. G. Debenedetti, J. Chem. Phys. **86**, 2229 (1987).

[13] P. H. Poole, F. Sciortino, U. Essmann, and H. E. Stanley, Nature (London) **360**, 324 (1992).

[14] G. M. Bell, J. Phys. C **5**, 889 (1972).

[15] P. H. E. Meijer, R. Kikuchi, and R. Papon, Physica A **109**, 365 (1982).

[16] S. S. Borick and P. G. Debenedetti, J. Phys. Chem. **97**, 6292 (1993).

[17] S. Sastry, F. Sciortino, and H. E. Stanley, J. Chem. Phys. **98**, 9863 (1993).

[18] S. Sastry, P. G. Debenedetti, F. Sciortino, and H. E. Stanley, Phys. Rev. E **53**, 6144 (1996).

[19] J. S. Walker and C. A. Vause, Phys. Lett. **79A**, 421 (1980).

[20] C. A. Vause and J. S. Walker, Phys. Lett. **90A**, 419 (1982).

[21] R. E. Goldstein and J. S. Walker, J. Chem. Phys. **78**, 1492 (1983).

[22] R. E. Goldstein, J. Chem. Phys. **79**, 4439 (1983).

[23] R. G. Caflish and J. S. Walker, Phys. Rev. B **28**, 2535 (1983).

[24] J. Lajzerowicz and J. Sivardiere, Phys. Rev. A **11**, 2079 (1975).

[25] Gangasharan, D. Kumar, and S. K. Sarkar, Phase Transit. **56**, 217 (1996).